PCCP

Accepted Manuscript

ROYAL SOCIETY OF CHEMISTRY

www.rsc.org/pccp

PCCP

RSCPublishing

COMMUNICATION

Mechanism of the S_1 Excited State Internal Conversion in Vitamin B_{12}

Cite this: DOI: 10.1039/x0xx00000x

Piotr Lodowski,[a] Maria Jaworska,[a] Tadeusz Andruniów, [b] Brady D. Garabato,[c] and Pawel M. Kozlowski[c*]

Received XXth XXXXX 2014,
Accepted XXth XXXXX 2014

DOI: 10.1039/x0xx00000x

www.rsc.org/

To explain the photostability of vitamin B_{12}, internal conversion of the S_1 state was investigated using TD-DFT. The active coordinates for radiationless deactivation were determined to be elongated axial bonds, overcoming a 5.0 kcal/mol energy barrier between the relaxed ligand-to-metal charge transfer (S_1), and the ground (S_0) states.

Derivatives of vitamin B_{12} (cyanocobalamin, CNCbl) (Fig. 1) are important bioinorganic cofactors,[1-3] that possess rich and complex photolytic properties mediated by their electronically excited states, that primarily depend upon the nature of their axial ligands.[4-19] In particular, alkylcobalamins such as methylcobalamin (MeCbl) or adenosylcobalamin (AdoCbl), undergo photodissociation upon excitation with light,[4-10] and in the case of MeCbl for example, the photolysis can be wavelength dependent.[11] Studies employing ultrafast transient absorption spectroscopy show that the time scale of alkylcobalamin excited state dynamics is in the range of femtoseconds to nanoseconds, and that the specific mechanism of photolysis depends not only on the type of alkyl group, but also the environment of the cofactor, such as solvent or enzyme.[12-15] Furthermore, in acidic conditions, when the lower axial dimethylbenzimidazole (DBI) base is replaced by water, a new channel for fast nonradiative decay is opened, and formation of a radical pair is followed by bond homolysis.[16]

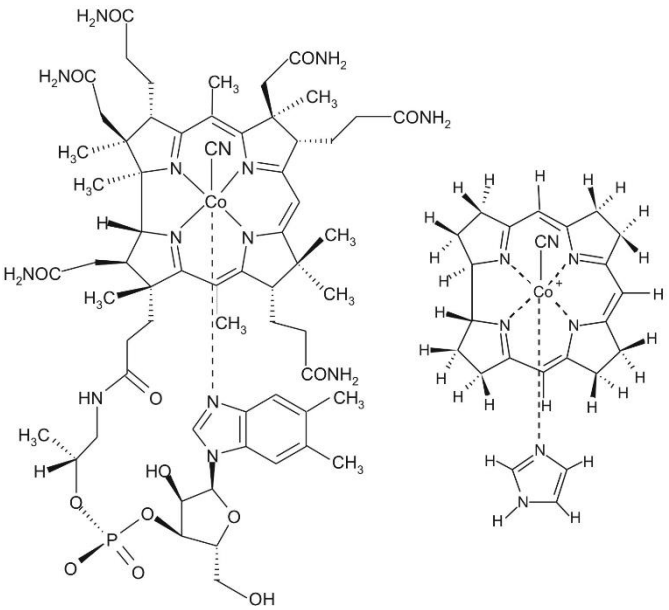

Fig. 1 (Left) Molecular structure of vitamin B_{12} (cyanocobalamin or CNCbl). (Right) Structural model of CNCbl used in this study, denoted as Im-[Co^{III}(corrin)]-CN^+.

In contrast, cobalamins with non-alkyl upper axial ligands are generally considered to be photostable.[17] Excitation of CNCbl, aquocobalamin (H_2OCbl^+), and azidocobalamin (N_3Cbl), results in the formation of a short-lived excited state that undergoes fast ground-state recovery on a picosecond time scale. The lifetime of the intermediate state decreases in the order, CNCbl > N3Cbl > H2OCbl$^+$, and also depends on the solvent, decreasing with the increased solvent polarity. Interestingly, although hydroxycobalamin (HOCbl) is a non-alkyl cobalamin, it undergoes photodissociation upon excitation with light above 300 nm.[18]

Ultrafast excited state dynamics in vitamin B_{12} revealed that, following 400 or 520 nm excitation, the intermediate state was formed within a few hundred femtoseconds.[17,19] The decay of this state to the ground state was temperature dependent, and ranged from 7.3 ps at 8° C to 5.7 ps at 63° C in water, and from 16.2 ps at 10° C to 8.1 ps at 75°C in ethylene glycol. The electronic spectrum of the short-lived intermediate was consistent with a weakening of both the axial Co-N_{DBI}, and Co-C bonds in the S_1 excited state. It was also found that the S_1 state has a predominantly $\pi \rightarrow 3d$ ligand-to-metal charge transfer (LMCT) character, with CT from the corrin π orbitals to the cobalt atom.[19] The barrier of internal conversion from S_1 to the ground state was determined to be 2.1 ± 0.2 kcal/mol in ethylene glycol, and 0.8 ± 0.2 kcal/mol in water, respectively.[19]

While excited-state dynamics of CNCbl have been extensively studied experimentally, there is a limited mechanistic understanding of its photostability. Previous theoretical investigations using DFT

and TD-DFT examined the nature of the lowest electronic transitions, and their corresponding potential energy surfaces (PESs).[20-21] The primary focus of these studies was on the electronic spectra of CNCbl, and the potential energy curves along the Co-C stretched bond. The S_1 PES as a function of axial bond distances, was also computed for the lowest excited states as vertical excitations based on their ground state geometries.[20]

To obtain a more realistic description of the S_1 PES, and thus more reliable energetics of the intermediates associated with the internal conversion (IC) mechanism, in the present theoretical account the excited state structural properties of CNCbl were investigated using TD-DFT.[22-26] The relaxed geometry of the S_1 state was constructed as a function of both axial Co-C and Co-N_{Im} distances, and a minimum energy crossing point with respect to the ground state was then located. These calculations were used to obtain a mechanism of S_1 state radiationless deactivation of vitamin B_{12}, that provide new insight at the molecular level into the excited state dynamics of CNCbl, in alignment with the latest experimental data.[19]

The computational methods used in this study are described fully in the Electronic Supporting Information (ESI). Briefly, all DFT and TD-DFT[26-27] calculations were performed in an implicit COSMO solvent model[28] using the BP86 functional,[29-30] and TZVPP basis set,[31-32] as implemented in TURBOMOLE.[33] The simplified structural model, denoted as Im-[Co^{III}(corrin)]-CN^+ (Fig. 1 and S1, ESI) used in this calculation, has proven to reproduce the essential structural and spectroscopic features of vitamin B_{12} very well.[20] The reliability of TD-DFT using the BP86 functional in the calculation of the lowest excited states for CNCbl was established in our previous studies.[20-21]

The DFT-based optimized geometry of the ground state (S_0) was in good agreement with x-ray crystallographic data (Tabe S1, ESI). In the S_1 state the Co-C bond is much longer than in the S_0 state (2.216 versus 1.857 Å). A similar trend was observed for the Co-N_{Im} bond, which was equal to 2.275 Å in the S_1 state, while 2.054 Å in the S_0 state. A characteristic weakening of the axial bonds of these ligands in the S_1 state was in agreement with previous experimental observation. The cyanide ligand was also slightly bent in the S_1 state (bending angle 170˚), in comparison with the linear arrangement in the ground state, while the geometry of the corrin ring remains essentially unchanged upon $S_0 \rightarrow S_1$ excitation. The NBO charge difference between the S_0 and S_1 electronic states calculated for the S_1 geometry (Table S2, ESI) shows a significant positive charge increase on the corrin ligand, and a negative charge increase on cobalt, cyanide and imidazole. Hence, the electron density is shifted from corrin to the axial ligands and cobalt. Similar conclusions can be drawn from the difference density between S_0 and S_1 isosurface plots (Fig. S2, SI), confirming the fully optimized S_1 state as being LMCT-type.

Because the nature of the low-lying excited states of Im-[Co^{III}(corrin)]-CN^+ have been analyzed previously, including their dependence on solvent, only a brief description will be given here. Analysis of the vertical electronic excitations revealed that the lowest transition is of $\pi \rightarrow \pi^*$ type. The second excited state (S_2) is of $\pi \rightarrow$d character, while S_3 and S_4 are a mixture of $\pi \rightarrow \sigma^*$ and π /d$\rightarrow \pi^*$ excitations. The higher electronic transitions are of mixed d$\rightarrow \pi^*$, π/d$\rightarrow \sigma^*$ and d$\rightarrow$d character (see Table S3, ESI). The optimized energy of the S_1 state as a function of Co-C distance is shown in Figure 2, where the energy of the vertical $\pi \rightarrow \pi^*$ excitation has been also included (denoted as A in Figure 2).

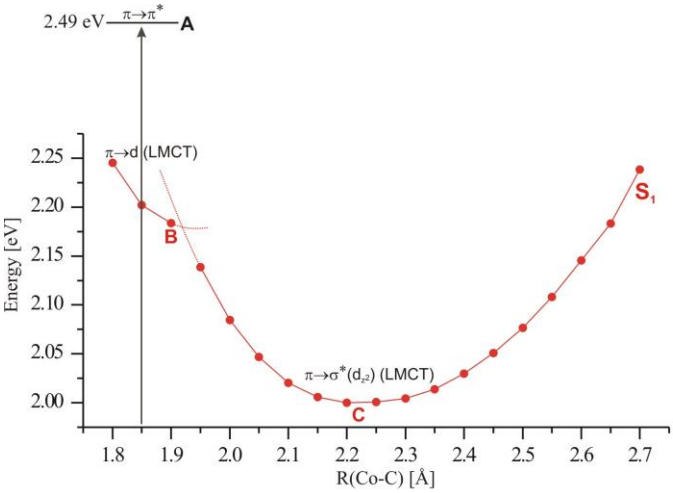

Fig. 2 Optimized energy of the S_1 state as function of the Co-C distance. Energy of the lowest vertical singlet excited state is denoted as A, and is based on the optimized geometry of the ground state. Point B corresponds to Co-C = 1.9 Å, while point C to the S_1 minimum.

The minimum energy at 2.216 Å is labeled as C, while the vicinity of crossing between two states that corresponds to the distance of 1.9 Å, is labeled as B. Note that crossing of two states along the Co-C coordinate can only be approximately estimated, and previous studies have demonstrated that this crossing may involve more than two electronic states.[21] It should be pointed out that the proposed mechanism is in accord with ultra-fast excited state dynamics, where an 80 fs decay of the initial excited state, a 190 fs decay of an intermediate electronic state, and a 6.7 ps decay of the S_1 excited state population to the ground state were reported.[17] These experimental time constants are consistent with the nature of the potential energy curves in Figure 2. To further understand the electronic properties of the excited states shown in Fig. 2, frontier orbitals corresponding to three different geometries, S_0 minimum (A), the optimized S_1 geometry corresponding to a Co-C distance of 1.9 Å (B), and the S_1 minimum geometry (C), were obtained from TD-DFT calculations (Fig. 3).

The lowest singlet excited state for all three geometries comes from the HOMO$\rightarrow$LUMO excitation. At the S_0 optimized geometry, the lowest S_1 excited state is of $\pi \rightarrow \pi^*$ character, as can be seen in the vertical electronic spectrum (Table S3, ESI). When the geometry of the S_1 state is optimized its character changes to $\pi \rightarrow$d/π even for the same Co-C distances corresponding to the minimum ground state. Around 1.9 Å, the character of S_1 becomes $\pi \rightarrow \sigma^*$. Since the antibonding σ^* orbital contains a large contribution from the d_z^2 cobalt orbital, the S_1 state at its optimal geometry can be described as a LMCT state with elongated, and weakened axial bonds, and is consistent with experimental assignment based on transient absorption spectroscopy.[19] These changes are also nicely reflected by the nature of the LUMO orbital (Fig. 3).

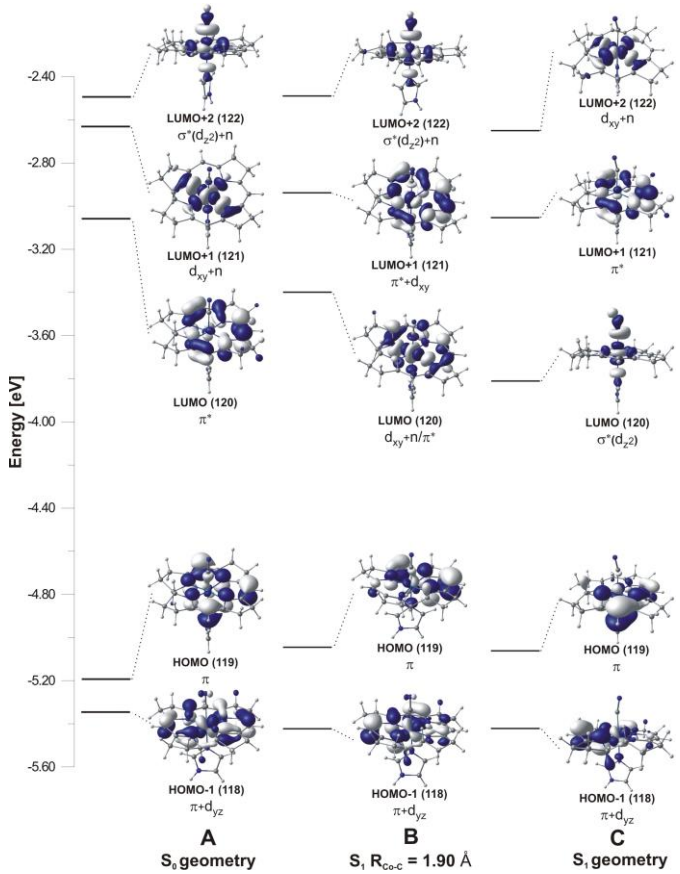

Fig. 3 Molecular orbital diagrams corresponding to the lowest singlet excited states of CNCbl representing; the optimized geometry of the S_0 state (A); the optimized geometry of the S_1 state with fixed Co-C bond distances at 1.9 Å (B); the optimized geometry of the S_1 state with fixed Co-C bond distances at 1.9 Å (B); the optimized geometry of the S_1 state (C).

Having discussed the properties of the low-lying electronic transitions along the Co-C stretched coordinate, we may now turn our attention to the properties of the PES associated with the S_1 state. The PES of the S_1 excited state of CNCbl was calculated based on the Im-[Co^{III}(corrin)]-CN^+ structural model (Fig. 1), and the energy of the excited state was optimized on a grid of points with different Co-C and Co-N_{Im} distances. Both bond distances were varied with a 0.05 Å step, while the remaining geometry parameters were optimized at each point with the TD-DFT method. The resulting S_1 energy surface as a function of optimized Co-C and Co-N_{Im} distances is displayed in Fig. 4, along with the upper portion of the ground state surface, where crossing with the S_0 state (i.e., the seam) is indicated by a black dashed line.

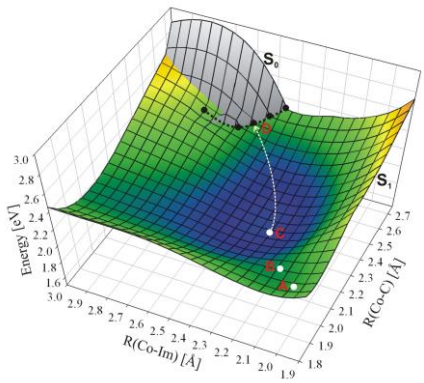

Fig. 4 Potential energy surface of the S_1 state, along with the upper portion of the ground state surface. Characteristic points on the S_1 PES correspond to: ground state S_0 geometry (A), S_1 with Co-C =1.9 Å (B); energy minimum of the S_1 state (C); minimum energy point of the S_1/S_0 crossing seam (D).

Note that the intersection seam was determined by extrapolation as will be described. There is a shallow minimum on the S_1 energy surface at Co-C = 2.216 Å, and Co-N_{Im} = 2.275 Å, that corresponds to the optimized structure of S_1. Starting from the vertical excitation of the S_0 geometry, labeled as A, there is a valley leading to the S_1 minimum, labeled as C (Fig. 4). Characteristic points A, B, C as well as the minimum energy crossing point (MECP) labeled as D, lie essentially on a diagonal cut bisecting the 3D PES. The corresponding energy curve along this minimum energy path between the S_0 and S_1 equilibrium geometries is presented in Fig. 5. As noticed previously, even for Co-C distances in the range 1.8-1.9 Å (Fig. 2), the lowest excited state is not a $\pi \rightarrow \pi^*$ state, but a $\pi \rightarrow$ d transition, indicating that during geometry optimization of the S_1 state the first and second electronic transitions are very close in energy, and change their order. At Co-C distances slightly larger than 1.9 Å, the crossing of two excited states occurs. This crossing is barrierless, since it happens before the minimum of the lowest singlet excited state, and changes its character to $\pi \rightarrow \sigma^*$. Thus, the changes in character of the S_1 state are the result of crossing between lowest excited states, which are close in energy.

Radiationless deactivation (or IC) of an excited state occurs when the excited and ground states cross with a small energy barrier, or no barrier at all. Interestingly, if one takes into consideration the diagonal cut (i.e., Fig. 5) through the 3D PES (Fig. 4) the resulting

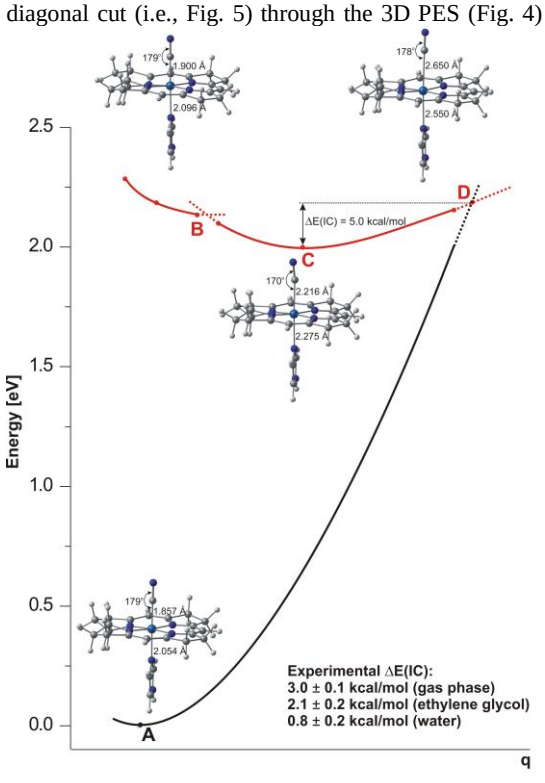

Fig. 5 Schematic representation of the diagonal cut bisecting the 3D PES, shown in Fig. 4.

energy path in fact can be associated with the S_1 excited state IC in CNCbl.

Near the points located on the intersection seam where the crossing of two electronic states takes place, the wavefunction should have a multi-configurational character, and such crossing of surfaces cannot be described appropriately by a single determinantal TD-DFT wavefunction. As a consequence, at the intersection points, problems with convergence of the SCF procedure appear.[34-35] Due to the size of CNCbl (~160 atoms), however, the TD-DFT method is the only choice to investigate their excited state properties, and this method was therefore applied in the present study. Not surprisingly, the calculation encounters convergence problems when the energy difference between the S_0 and S_1 states becomes ~2 kcal/mol. To circumvent these problems that are inherent in TD-DFT methodology, quadratic extrapolation was used to estimate the intersection point. The coordinates active in the S_1/S_0 internal conversion were determined to be only Co-C and Co-N_{Im} distances, because these coordinates differ mostly in the optimized structures of the S_0 and S_1 states. This can be deduced from the fact that when both distances were elongated, the S_1 and S_0 surfaces approach each other. Other coordinates, like Co-C-N_{Im} bending angle, and selected corrin bending or torsional angles were also varied, but the excitation energy remained essentially constant. The minimum energy point on the seam was taken as the intersection point, labeled D, and the resulting energy barrier between the S_1 minimum, and the minimum on the intersection seam was determined to be ~5.0 kcal/mol. The energy of 5.0 kcal/mol can be directly compared to a 2.1 ± 0.2 kcal/mol experimental IC barrier based on the dielectric constant of 80 at room temperature for water.[19] The estimated energy barrier of 5.0 kcal/mol (Fig. 5) has to be taken with caution, due to the method of searching for the S_0/S_1 crossing point. The overestimation of its height is due to several possible sources of error: (1) the extrapolation procedure has an associated error which can estimated to be around 2 kcal/mol, (2) only a limited number of parameters were taken into account in the search for the lowest energy crossing point. Although increasing the number of parameters (over three) could possibly lower the energy of the crossing, the calculations would not be feasible. (3) The accuracy of the computational method itself associated with TD-DFT also represents a limiting factor. (4) There may also be additional computational error associated with the solvent model, in accord with experiments that suggest the barrier is also sensitive to solvent polarity-- though this may be the least significant source of error comparatively. By taking all of these factors into account, the calculated energy barrier can be viewed as quite satisfactory in comparison with experimental value.

Based on a diagonal cut through the 3D PES (Fig. 4), which shows how the S_1 and S_0 energy surfaces cross (Fig. 5), the following mechanism of radiationless deactivation of the S_1 state in CNCbl can be proposed. After initial excitation to one of the higher-lying excited states, a fast reversion to the lowest $\pi \rightarrow \sigma^*$ excited state takes place. Next the system goes through an intermediate state of $\pi \rightarrow$d character, and eventually reaches the S_1 minimum of $\pi \rightarrow \sigma^*$ character. This process is very fast and can be ascribed to the femtosecond time range of CNCbl photophysics.[19] This process is also barrierless, and the crossing with the intermediate state occurs before reaching the minimum of the first excited state. The lifetime of the lowest excited state of CNCbl can be estimated to be between 2 - 16 ps.[19] By analyzing the minimum energy path leading from the vertically excited S_0 geometry (A), to the minimum on the S_1 PES (C), and finally to the lowest energy point on the crossing seam between S_0 and S_1 (D), it can be seen that along this path both axial bonds are simultaneously elongated. The geometry of the crossing point, shown in Fig. 5, has very long axial bond distances: 2.65 Å for Co-C and 2.55 Å for Co-N_{Im}. The cyanide ligand is practically linear, revealing that the Co-C bending angle has no impact on the energy of the intersection point. This is understandable since at such a long distances the cyanide ligand is weakly bound, and bending does not influence the total energy of the molecule.

Conclusions

In summary, the ground-state recovery process in CNCbl can be described as excitation to one of the higher-lying excited states, initial relaxation to the corresponding S_1 excited state geometry, and further electronic state relaxation on the S_1 energy surface until the minimum on this surface is attained, and crossing the energy barrier of the S_1/S_0 intersection. To overcome this energy barrier, elongation of the axial bonds in CNCbl is required, that according to our calculations are the active coordinates for the radiationless deactivation of the S_1 state.

Acknowledgements

This work was financed by a statuary activity subsidy from the Polish Ministry of Science and Higher Education for the Faculty of Chemistry of Wroclaw University of Technology (TA). TURBOMOLE calculations were carried out in the Wroclaw Centre for Networking and Supercomputing, WCSS, Wroclaw, Poland, http://www.wcss.wroc.pl, under calculational grant No. 18 and in the Academic Computer Centre CYFRONET of the University of Science and Technology in Cracow, ACC CYFRONET AGH, Kraków, Poland, http://www.cyfronet.krakow.pl, under grants MNiSW/ SGI3700/ USląski/ 111/2007 and MNiSW/ IBM_BC_HS21/ USląski/ 111/2007. We also acknowledge a statutory activity subsidy from the National Science Centre, Poland, under grant No. UMO-2013/09/B/ST4/03014.

Notes and references

[a] Department of Theoretical Chemistry, Institute of Chemistry, University of Silesia, Szkolna 9, PL-40 006 Katowice, Poland.
[b] Institute of Physical and Theoretical Chemistry, Department of Chemistry, Wroclaw University of Technology, 50-370 Wroclaw, Poland.
[c] Department of Chemistry, University of Louisville, Louisville, Kentucky 40292, USA..

† Electronic Supplementary Information (ESI) available: [(i) computational details, (ii) selected geometrical parameters of optimized geometries for the ground (S_0) and excited (S_1) states, (iii) NBO charges for S_0 and S_1 optimized geometries, (iv) ten lowest electronically excited states, vertical singlet electronic transitions for Im-[Co^{III}(corrin)]-CN^+ model complex based on the TD-DFT calculations, (v) structural model of CNCbl used in calculations, (vi) isosurface and cross-section contour of electron density difference between the S_1 and S_0 states for the S_1 optimized geometry of CNCbl model]. See DOI: 10.1039/c000000x/

1 Dolphin, D. Ed. B_{12}; John Wiley & Sons: New York, 1982.

2 B. Kräutler, D. Arigoni, B. T. Golding, Ed. Vitamin B_{12} and B_{12} Proteins; Wiley-VCH: New York, 1998.
3 R. Banerjee, Ed. Chemistry and Biochemistry of B_{12}; John Wiley & Sons: New York, 1999.
4 G. N. Schrauzer, L. P. Lee, J. W. Sibert *J. Am. Chem. Soc*. 1970, **92**, 2997–3005.
5 E. Chent, M. R. Chance, *Biochemistry*, 1993, **32**, 1480-1487.
6 J. T. Jarrett, C. L. Drennan, M. Amaratunga, J. D. Scholten, M. L. Ludwig, R. G. Matthews, *Bioorganic & Medicinal Chemistry*. 1996, **4**, 1237-1246.
7 B. H. Zhu, Z. H. Liu, H. Yan, J. Liu, H. Chen, *J. Inor. Biochem*, 1997, **65**, 45-52.
8 W. D. Robertson, K. Warncke, *Biochemistry*, 2009, **48**, 140–147
9 L. A. Walker II, J. T. Jarrett, N. A. Anderson, S. H. Pullen, R. G. Matthews, R. J. Sension, *J. Am. Chem. Soc.*, 1998, **120**, 3597-3608.
10 L. A. Walker II, J. J. Shiang, N. A. Anderson, S. H. Pullen, R. J. Sension, *J. Am. Chem. Soc*., 1998, **120**, 7286-7292.
11 J. J. Shiang, L. A. Walker II, N. A. Anderson, A. G. Cole, R. J. Sension, *J. Phys. Chem. B*, 1999, **103**, 10532-10539.
12 L. M. Yoder, A. G. Cole, L. A. Walker II, R. J. Sension, *J. Phys. Chem. B*, 2001, **105**, 12180-12188.
13 A. G. Cole, L. M. Yoder, J. J. Shiang, N. A. Anderson, L. A. Walker II, M .M. Banaszak Holl, R. J. Sension, *J. Am. Chem. Soc*., 2002, **124**, 434-441.
14 R. J. Sension, D. A. Harris, A. Stickrath, A. G. Cole, C. C. Fox, E. N. G. Marsh, *J. Phys. Chem. B*, 2005, **109**, 18146-18152.
15 R. J. Sension, D. A. Harris, A. G. Cole, *J. Phys. Chem. B*, 2005, **109**, 21954-21962.
16 J. Peng, K.-C.Tang, K. McLoughlin, Y. Yang, D. Forgach, R. J. Sension, *J. Phys. Chem. B*, 2010, **114**, 12398–12405.
17 J. J. Shiang, A. G. Cole, R. J. Sension, K. Hang, Y. Weng, J. S. Trommel, L. G. Marzilli, T. Lian,, *J. Am. Chem. Soc*., 2006, **128**, 801-808.
18 T. A. Shell, D. S. Lawrence, *J. Am. Chem. Soc.*, 2011, **133**, 2148-2150.
19 D. A. Harris, A. B. Stickrath, E. C. Carroll, R. J. Sension, *J. Am. Chem. Soc*., 2007, **129**, 7578-7585.
20 P. Lodowski, M. Jaworska, K. Kornobis, T. Andruniów, P. M. Kozlowski, *J. Phys. Chem. B*, 2011, **115**, 13304–13319.
21 K. Kornobis, N. Kumar, B. M. Wong, P. Lodowski, M. Jaworska, T. Andruniów, K. Ruud, P. M. Kozlowski, *J. Phys. Chem. A*, 2011, **115**, 1280– 1292.
22 E. J. Baerends, G.Ricciardi, A. Rosa, S. J. A. van Gisergen, *Coor. Chem. Rev.*, 2002, **230**, 5–27.
23 A. Rosa, G. Ricciardi, O. Gritsenko, E. J. Baerends, 49-116 in: N. Kaltsoyannis, J. E. McGrady, Principles and Applications of Density Functional Theory in Inorganic Chemistry I, **112**, Structure and Bonding; Springer-Verlag: Berlin Heidelberg, 2004.
24 A. Dreuw, M. Head-Gordon, *Chem. Rev*., 2005, **105**, 4009–4037.
25 A. Dreuw, *ChemPhysChem*, 2006, **7**, 2259–2274.
26 E. Runge, E. K. U. Gross, *Phys. Rev. Lett.*, 1984, **52**, 997–1000.
27 M. E. Casida, 391-439: J. M. Seminario, ed. Recent Developments and Application of Modern Density Functional Theory; Elsevier: Amsterdam, 1996.
28 A. Klamt, G. Schüürmann, *J. Chem. Soc*., Perkin Trans. 1993, **2**, 799-805
29 A. D. Becke, *Phys. Rev. A*, 1988, **38**, 3098-3100.
30 J. P. Perdew, *Phys. Rev. B*, 1986, 33, 8822-8824.
31 F. Weigend, M. Häser, H. Patzelt, R. Ahlrichs, *Chem. Phys. Lett*., 1998, **294**, 143–152.
32 K. Eichkorn, F. Weigend, O. Treutler, R. Ahlrichs, *Theor. Chem. Acc*., 1997, **97**, 119-124.
33 (a) R. Ahlrichs, M. Bär, M. Häser, H. Horn, C. Kölmel, *Chem. Phys. Lett.*, 1989, **162**, 165-169. (b) O. Treutler, R. Ahlrichs, *J. Chem. Phys.*, 1995, **102**, 346-354. (c) F. Furche, R. Ahlrichs, *J. Chem. Phys.*, 2002, **117**, 7433-7447. (d) F. Furche, D. Rappoport, Theoretical and Computational Chemistry, **16**, Elsevier, Amsterdam, 2005. (e) TURBOMOLE has been designed by the Quantum Chemistry Group, University of Karlsruhe, Germany, since 1988. The following members of the group have made contributions: R. Ahlrichs, M. Bär, H.-P. Baron, R. Bauernschmitt, S. Böcker, N. Crawford, P. Deglmann, M. Ehrig, K. Eichkorn, S. Elliott, F. Furche, F. Haase, M. Häser, C. Hättig, A. Hellweg, H. Horn, C. Huber, U. Huniar, M. Kattannek, A. Köhn, C. Kölmel, M. Kollwitz, K.s May, P. Nava, C. Ochsenfeld, H. Öhm, H. Patzelt, D. Rappoport, O. Rubner, A. Schäfer, U. Schneider, M. Sierka, O. Treutler, B. Unterreiner, M. von Arnim, F. Weigend, P.Weis, H. Weiss, http://www.turbomole.com
34 J. Plötner, A. Dreuw, *J. Phys. Chem. A*, 2009, **113**, 11882–11887.
35 R. Improta, F. Santoro, *J. Phys. Chem. A*, 2005, **109**, 10058-10067.